EFFECTS OF A WAVY NEUTRAL SHEET ON COSMIC RAY ANISOTROPIES

J. Kóta (1,2) and J.R. Jokipii (1)
(1) The University of Arizona, Tucson, Arizona, USA
(2) Central Research Institute for Physics, Budapest, Hungary

Abstract. We present the first results of our 3-D numerical code calculating cosmic ray anisotropies. The code includes diffusion, convection, adiabatic cooling, and drift in an interplanetary magnetic field model containing a wavy neutral sheet. We find that the 3-D model can reproduce all the principal observations for a resonable set of parameters.

Introduction. In the last decade, the effects of curvature and gradient drifts became a central issue in the theory of cosmic ray transport. It has been suggested that drift may play an important, and perhaps dominant, role in cosmic ray propagation in the heliosphere, and it may be responsible for the asymmetries appearing in consecutive 11-year cycles (Jokipii, Levy and Hubbard 1977; Jokipii and Kopriva 1980; Kóta 1979; Jokipii and Thomas 1981; Kóta and Jokipii 1983). The first success of drift models in explaining galactic cosmic-ray phenomena was the explanation of the phase shift of the solar daily variation (Levy 1976) observed in the years of the seventies, following the polarity reversal of the solar magnetic field. The first quantitative 2-dimensional (2-D) calculation was carried out by Jokipii and Kopriva (1980). In this work, however, the too small value of the diffusion coefficient, κ, led to unreasonable anisotropies in some cases. Kóta (1981) derived an approximate force-field solution with a virtually perfect isotropy. This model, however, relied upon the too simple picture of 'hard-sphere' scattering.

The well known phase shift of the solar daily variation (Duggal and Pomerantz, 1975) is naturally explained by 2-D models (Levy 1976, Kadokura and Nishida 1984). The magnetic configuration of the seventies (A>0) yields a smaller radial density gradient which cannot balance the convection by the solar wind and thus results in a net outward streaming. Another well established observation is the presence of the polarity dependent N-S anisotropy associated with the $\underline{B} \times \underline{\nabla} n$ streaming (Bercovitch 1970, Pomerantz and Bieber 1984). In the seventies (A>0), this streaming is directed away from the neutral sheet. In a 2-D model, this pattern of streaming is hard to reconcile with the div $\underline{S} < 0$ requirement, thus 2-D models are bound to encounter difficulties in explaining both observations.

The basic difficulty, in principle at least, may be removed if, violating the axial and N-S symmetries, a wavy neutral sheet is included. It is the purpose of this work to demonstrate that a 3-D model is indeed able to reproduce all components of the observed anisotropies. We present the first anisotropy results of our 3-D code incorporating a wavy neutral sheet.

The Model. We used a 3-D numerical code to solve the modulation equation including diffusion, convection, adiabatic deceleration and drift. The model and the scheme of calculation were described in detail elsewhere (Kóta and Jokipii 1983, see also the preceding paper SH-4.2-10 in this issue). Briefly, a usual spiral field is adopted, the magnetic equator is a tilted plane at the sun, which then evolves into a wavy sheet (Jokipii and Thomas 1981). The case of A>0 corresponds to outward polarity above

the sheet and inward polarity below the sheet while A<0 corresponds to the opposite configuration (sixties and eighties). Steady state is assumed in the frame corotating with the sun. The most serious limitation of the code is that it assumes constant solar wind speed thus many phenomena, like shocks, are precluded.

Calculations were carried out for protons in the 1 - 10 GV range. The parallel diffusion coefficient, $\kappa_{\parallel}$, was assumed to be inversely proportional to the magnetic field strength, B,

$$\kappa_{\parallel} = K_0 P^{1/2} \beta \, (B_{earth}/B)$$

with P being the particle rigidity in GV, β is the particle velocity in units of velocity of light, and K_0 is a normalization constant in the range of $10^{21} - 10^{23}$ cm^2/sec. The ratio of the perpendicular and parallel diffusion coefficients was kept constant at $\kappa_{\perp}/\kappa_{\parallel}$ =0.05-0.20.

Results and Discussion. Anisotropies were calculated at three heliocentric distances (0.5, 1, and 5 AU) over the full range of heliographic latitudes and longitudes. Here, we present the results near the earth. The anisotropies to be reported are obtained at the helioequator, at 1 AU, and averaged over longitudes in a magnetic sector.

The ecliptic components of the anisotropy responsible for the solar daily variation are given in Figures 1 and 2 (P=2.3 GV; $\kappa_{\perp}/\kappa_{\parallel}$ =.05). It should be noted that the anisotropies obtained for a flat sheet (dashed lines) show sharp changes at the neutral sheet. The actual values (dots) may considerably differ from the averages over a (-5°, 5°) latitude band (open circles). In most cases, A>0 gives an earlier phase and a smaller amplitude which is in general agreement with observations. Similar results were obtained for other rigidities, too. At large values of K_0, understandably, drift effects diminish and a near perfect corotation applies. The breaks in the lines in the $K_0 = 1.5\text{-}5.10^{22}$ cm^2/sec range indicate that corotation should be reached somewhere in this interval.

Figure 3 shows ξ_{ϑ}, the zenith angle component of the average near earth anisotropy above the neutral sheet for P = 2.3 GV. Consider first the case A>0, when the 'observed' value of ξ_{ϑ} is negative in accordance with the sense of the $\underline{B} \times \underline{\nabla} n$ streaming. Curve (a) corresponding to $\kappa_{\perp}/\kappa_{\parallel}$ = .05 and α = 15° yields the correct sign for ξ_{ϑ}. Larger tilt angle (α = 30°, curve (b)), however, may already give positive values, too. If we take, on the other hand, a larger perpendicular diffusion (curve (c): $\kappa_{\perp}/\kappa_{\parallel}$=.20, α=30°) ξ_{ϑ} will again point in the proper direction for all values of K_0. The underlying physical picture is that, in the case of large tilt angles and small perpendicular diffusion, most particles reach the earth without having interacted with the neutral sheet. Being too far from the earth, the neutral sheet becomes irrelevant for A>0. As for A<0, particles intersect the sheet several times before reaching the earth. As a result, the calculated ξ_{ϑ} always shows the proper sense and is fairly independent of the tilt angle, α.

Figure 4 indicates that the magnitude of ξ_{ϑ} increases and its sign becomes more distinctive with increasing rigidities. This finding can also be anticipated since drift effects are expected to be more pronounced at higher rigidities.

The typical azimuthal dependence of the N-S anisotropy is presented in Figure 5. In most cases, we cannot find a one-to-one correspondence between the sign of ξ_{ϑ} and the polarity of the field. In general, smaller tilt angle, and larger $\kappa_{\perp}$ results in a better correlation; the

correlation also improves at higher rigidities. At 5 AU heliocentric distance, virtually all our runs gave a 100 percent correlation. To interpret this, we note that the waves in the neutral sheet become relatively tighter at larger distances from the sun. Thus we expect the effects of waviness to be more direct there.

Conclusion. Our numerical results demonstrate that the inclusion of a wavy neutral sheet may explain all components of the observed anisotropies. We find a general agreement between 'theoretical' and 'observed' anisotropies for a wide range of parameters. At high latitudes, well above or below the sheet, however, we predict the anisotropy to point toward the equator in the case of A>0. This is in contrast to the poleward direction expected from the $\underline{B} \times \nabla n$ term only.

Acknowledgement. This work was supported by the National Science Foundation under Grants ATM-220-18 and INT-8400591.

References.

Bercovitch, M. 1970: Acta Phys. Hung., 29, Suppl 2, 169
Duggal, S. P. and Pomerantz, M. A. 1975: Proc. 14th ICRC, Munich, 4, 1209
Jokipii, J. R. and Kopriva, D. A. 1980: Ap. J., 234, 384
Jokipii, J. R. and Thomas, B. T. 1981: Ap. J., 243, 1115
Jokipii, J. R., Levy, E. H. and Hubbard, W. B. 1977: Ap. J., 213, 861
Kota, J. 1979: Proc. 16th ICRC, Kyoto, 3, 13
Kota, J. 1981: Adv. Space Res., 1, no. 3, 135
Kota, J. and Jokipii, J. R. 1983: Ap. J., 265, 573
Levy, E. H. 1976: J. Geophys. Res., 81, 2082
Kadokura, A. and Nishida, A. 1984: Proc. Int. Symp. on CR Modulation, Morioka, Japan 1984, p177
Pomerantz, M. A. and Bieber, I. W. 1984: Proc. Int. Symp. on CR Modulation, Morioka, Japan 1984, p39

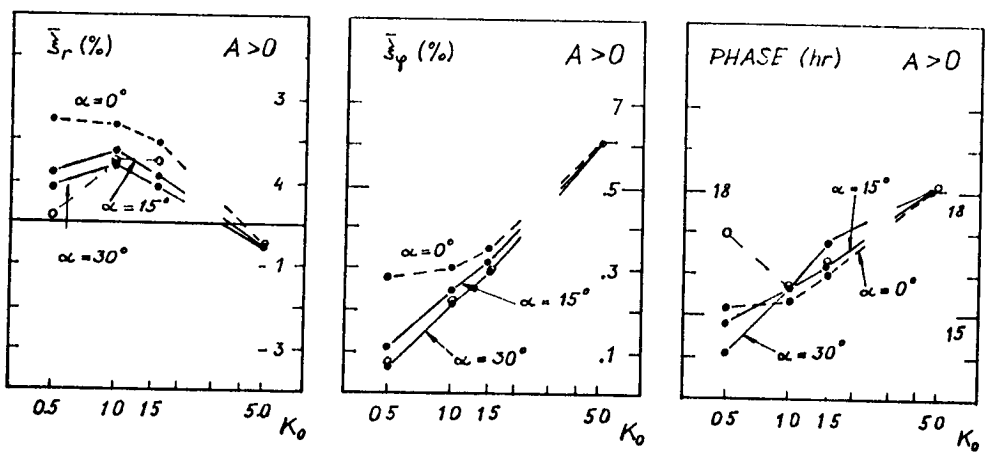

Figure 1. Radial and azimuthal components of the average near earth anisotropy calculated for A>0, P=2.3 GV, $\kappa_\perp/\kappa_\parallel$=.05. Dashed and solid lines refer to flat (see text) and wavy sheets, respectively. K_0 is in units of 10^{22} cm^2/sec. The phases of the resulting daily waves are also shown.

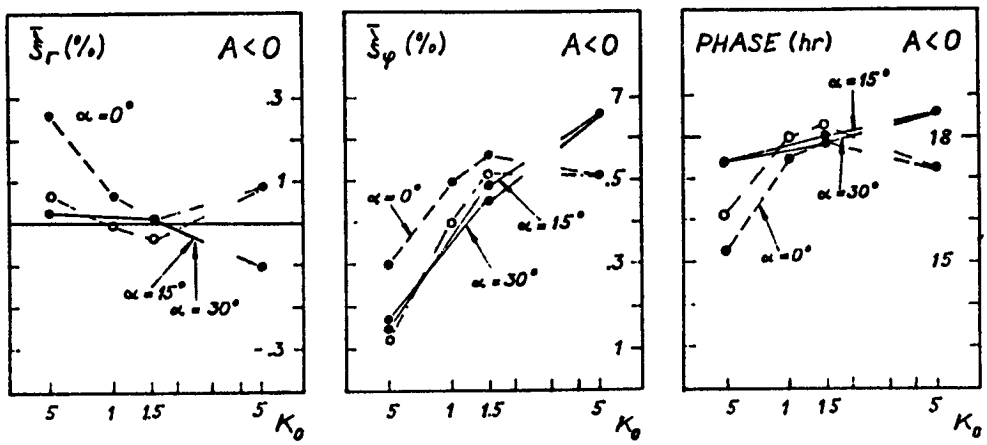

Figure 2. Same as Fig. 1., for A<0.

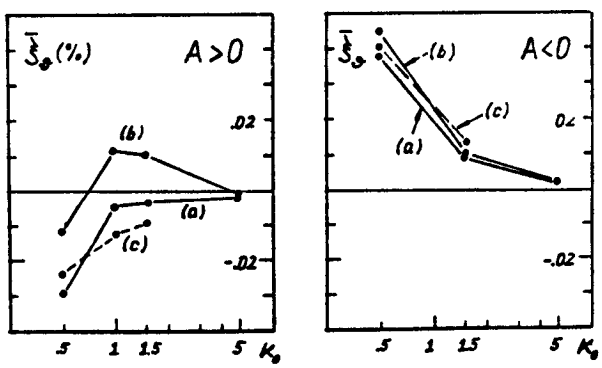

Figure 3. The average value of ξ_ϑ for the earth being above the neutral sheet. P=2.3 GV, K_0 is in units of 10^{22} cm^2/sec.
(a) $\kappa_\perp/\kappa_\parallel$=.05, α =15°;
(b) $\kappa_\perp/\kappa_\parallel$=.05, α =30°;
(c) $\kappa_\perp/\kappa_\parallel$=.20, α =30°.

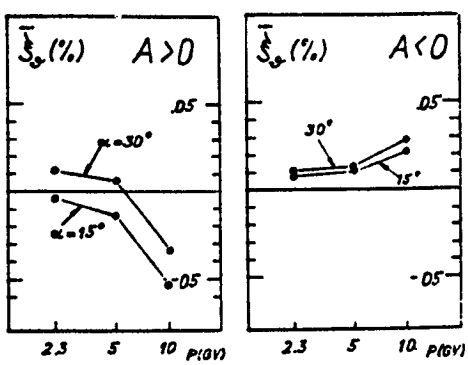

Figure 4. ξ_ϑ vs rigidity calculated for $K_0=10^{22}$ cm^2/sec, $\kappa_\perp/\kappa_\parallel$=0.05.

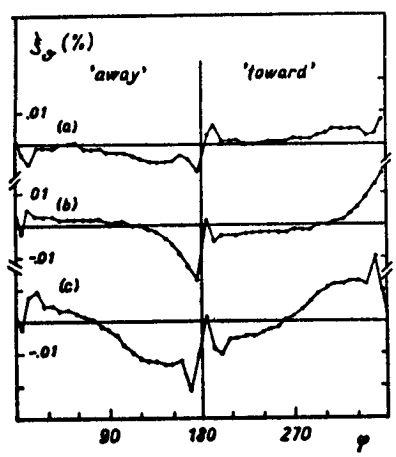

Figure 5. Azimuthal dependence of ξ_ϑ calculated for P=2.3 GV, $\kappa_\perp/\kappa_\parallel$=.05.
(a) A>0, α=15°; (b) A>0, α=30°;
(c) A<0, α=15°.